Analysis of damping forces exerted by single-component gases and mixtures in high-frequency MEMS devices

Silvia Lorenzani
Dipartimento di Matematica, Politecnico di Milano, Italy
E-mail: silvia.lorenzani@polimi.it

Keywords: MEMS devices, damping forces, Boltzmann equation.

SUMMARY. In the present paper, we analyze the mechanism leading to gas damping in micro-electro-mechanical systems devices vibrating at high frequencies through the linearized Boltzmann equation based on a simplified kinetic model and diffuse reflection boundary conditions.

1 INTRODUCTION

Radio frequency micro-electro-mechanical systems (RF MEMS) devices have been identified as a technology that has the potential to provide a major impact on existing RF architectures in sensors and communications. Over the last decade, RF MEMS (ranging from 1 MHz to 60 GHz) have become a key research area because they should enable a miniaturization and an integration of RF components by reducing weight, cost, size and power dissipation, with applications to ultra low-power wireless and adaptive/secure telecommunications [1], [2], [3]. In particular, the development of integrated silicon-based micromechanical resonators with high frequencies and high quality factors can have a great impact on the future of wireless communication systems. Due to the high stiffness of RF micromechanical resonators, the ratio of the energy lost by the air damping to the stored energy is much smaller compared to that of the flexural mode of lower frequency beam resonators. The high quality factors maintained by RF disk resonators at atmospheric pressure indicate the potential of these microdevices for several applications and implementation in wireless systems without the need for expensive vacuum packaging. So far, in all the works where a mechanical analysis of RF MEMS has been reported, it was stressed that these devices are able to maintain high quality factors even at atmospheric pressure due to their much higher stiffness in comparison to other types of resonators vibrating at low frequencies. Indeed, when MEMS devices vibrate at high frequencies also the gas damping mechanism changes compared to that experienced by low frequency MEMS. An important class of commercial microdevices is represented by silicon inertial sensors and actuators produced by surface micromachining processes, like accelerometers and gyroscopes. Such devices, working at a relatively low frequency, are normally operated at very low pressure in order to minimize the damping due to the internal friction of the gas (viscous damping). This need can be overcome when MEMS devices vibrate at relatively high frequencies, since gas compressibility and inertial forces lead then to another damping mechanism which is related to the propagation of sound waves generated by high-frequency oscillating micro-structures. In this frame, it is important to analyze not only the damping forces exerted by single-component gases but also those exerted by gas mixtures, since during the wafer bonding process a mixture of noble gases (like Ar, Kr or Ne) and getterable gases (like N_2, O_2 or CO_2) is usually backfilled into the MEMS sensor package to set its operating pressure ('backfilling process').

In the current investigation, by using the linearized Boltzmann equation based on simplified kinetic models, we prove that, for a single-component gas and for mixtures (like Ne-Ar) whose constituents have comparable molecular mass, the sound waves propagating between the microdevice walls induce a resonant/antiresonant response of the system. The occurrence of an antiresonance

is particularly important since if the device is operated close to the corresponding frequency, the damping due to the gas is considerably reduced. Completely different behaviour has been detected, in the near-continuum regime, for disparate-mass gas mixtures (composed of very heavy plus very light molecules) like He-Xe.

2 PROBLEM FORMULATION

Let us consider a binary gaseous mixture confined between two flat, infinite, and parallel plates located at $z' = -d/2$ and $z' = d/2$. Both boundaries are held at the same constant temperature. The upper wall of the channel (located at $z' = d/2$) is fixed while the lower one (located at $z' = -d/2$) harmonically oscillates in the z'-direction (normal to the wall itself) with angular frequency ω' (the corresponding period being $T' = 2\pi/\omega'$). The velocity U'_w of the oscillating plate depends on time t' through the formula: $U'_w(t') = U'_0 \sin(\omega' t')$, where it is assumed that the amplitude U'_0 is very small compared to the characteristic molecular velocity of the mixture given by $v_0 = \sqrt{2kT_0/m}$, with k being the Boltzmann constant, m being the mean molecular mass of the mixture and T_0 being the equilibrium temperature of the mixture. Under these conditions, the Boltzmann equation modeling the gaseous mixture motion inside the channel can be linearized by representing the distribution function of each species, f^s, as follows

$$f^s = f_0^s(1 + h^s), \qquad |h^s| << 1\,, \tag{1}$$

where h^s is the small perturbation with respect to the equilibrium state and f_0^s is the Maxwellian configuration given by

$$f_0^s = n_0^s \left(\frac{m^s}{2\pi k T_0}\right)^{3/2} \exp\left[-\frac{m^s}{2kT_0}|\xi - \mathbf{v_0}|^2\right] \tag{2}$$

with some common temperature T_0 and velocity $\mathbf{v}_0$ (which can be assumed equal to zero without loss of generality). In Eq. (2), n_0^s represents the equilibrium number density and m^s denotes the molecular mass.

Then, the system of linearized Boltzmann equations based on a simplified kinetic model of BGK-type after the projection reads ([4]):

$$\begin{aligned}\frac{\partial H^1}{\partial t} + c_z\,\frac{\partial H^1}{\partial z} + H^1 &= \rho^1 + 2(1-\Gamma^1)\,c_z\,v_z^1 + 2\Gamma^1 c_z\,v_z^2 \\ &+ \left[1 - \frac{2\Gamma^1 M_{12}}{(1+M_{12})}\right](c_z^2 - \tfrac{1}{2})\,\tau^1 + \frac{2\Gamma^1 M_{12}}{(1+M_{12})}(c_z^2 - \tfrac{1}{2})\,\tau^2\end{aligned} \tag{3}$$

$$\begin{aligned}\frac{\partial H^2}{\partial t} + c_z\,\frac{\partial H^2}{\partial z} + \Theta_{12}H^2 &= \Theta_{12}\Bigg\{\rho^2 + \frac{2(1-\Gamma^2)}{M_{12}}\,c_z\,v_z^2 + \frac{2\Gamma^2}{M_{12}}c_z\,v_z^1 \\ &+ \left[1 - \frac{2\Gamma^2}{(1+M_{12})}\right]\left(\frac{c_z^2}{M_{12}} - \tfrac{1}{2}\right)\tau^2 + \frac{2\Gamma^2}{(1+M_{12})}\left(\frac{c_z^2}{M_{12}} - \frac{1}{2}\right)\tau^1\Bigg\}\end{aligned} \tag{4}$$

$$\frac{\partial \Psi^1}{\partial t} + c_z\,\frac{\partial \Psi^1}{\partial z} + \Psi^1 = \left[1 - \frac{2\Gamma^1 M_{12}}{(1+M_{12})}\right]\tau^1 + \frac{2\Gamma^1 M_{12}}{(1+M_{12})}\tau^2 \tag{5}$$

$$\frac{\partial \Psi^2}{\partial t} + c_z\,\frac{\partial \Psi^2}{\partial z} + \Theta_{12}\Psi^2 = \Theta_{12}\left\{\left[1 - \frac{2\Gamma^2}{(1+M_{12})}\right]\tau^2 + \frac{2\Gamma^2}{(1+M_{12})}\tau^1\right\} \tag{6}$$

where all variables have been rescaled as follows: $t = t'/\theta_1$, $z = z'/(v_0^1\theta_1)$ with $v_0^1 = \sqrt{2kT_0/m^1}$, and $\Theta_{12} = \theta_1/\theta_2 = \nu_2/\nu_1$. The values of collision frequencies ν_1, ν_2 are determined by imposing that the linearized BGK model reproduces the linearized exchange rates for the viscous stress tensors prescribed by Boltzmann equations. Skipping calculation details, such a constraint yields

$$\Theta_{12} = \left[\sqrt{\frac{\eta^1}{\eta^2}}\,\sqrt{M_{12}}\,\sqrt{1+M_{12}} + \sqrt{2}\,M_{12}\,N_{12}\right]\left[\sqrt{\frac{\eta^2}{\eta^1}}\,\sqrt{M_{12}}\,\sqrt{1+M_{12}}\,N_{12} + \sqrt{2}\right]^{-1} \tag{7}$$

where η^s ($s = 1, 2$) are the viscosity coefficients of the two species, $M_{12} = m^1/m^2$ is the mass ratio and $N_{12} = n_0^1/n_0^2$ is the equilibrium concentration ratio. Furthermore, the coefficients Γ^1, Γ^2 appearing in Eqs. (3)-(6) are given by

$$\Gamma^1 = \frac{2}{3}\,\frac{A_1(5)}{A_2(5)}\left[1 + N_{12}\sqrt{\frac{\eta^2}{\eta^1}\,\frac{\sqrt{M_{12}}}{2}}\,\sqrt{1+M_{12}}\right]^{-1} \tag{8}$$

$$\Gamma^2 = \frac{2}{3}\,\frac{A_1(5)}{A_2(5)}\left[1 + N_{12}^{-1}\sqrt{\frac{\eta^1}{\eta^2}\,\frac{1}{2\,M_{12}^{3/2}}}\,\sqrt{1+M_{12}}\right]^{-1} \tag{9}$$

where $A_1(5) \simeq 0.422$ and $A_2(5) \simeq 0.436$ are the dimensionless collision cross sections reported in [5]. In Eqs. (3)-(6), the reduced unknown distribution functions H^s and Ψ^s are defined as

$$H^1(z, c_z, t) = \frac{1}{\pi}\int_{-\infty}^{+\infty}\int_{-\infty}^{+\infty} h^1(z, \mathbf{c}, t)\, e^{-(c_x^2+c_y^2)}\, dc_x\, dc_y \tag{10}$$

$$H^2(z, c_z, t) = \frac{1}{\pi M_{12}}\int_{-\infty}^{+\infty}\int_{-\infty}^{+\infty} h^2(z, \mathbf{c}, t)\, e^{-(c_x^2+c_y^2)/M_{12}}\, dc_x\, dc_y \tag{11}$$

$$\Psi^1(z, c_z, t) = \frac{1}{\pi}\int_{-\infty}^{+\infty}\int_{-\infty}^{+\infty} (c_x^2 + c_y^2 - 1)\, h^1(z, \mathbf{c}, t)\, e^{-(c_x^2+c_y^2)}\, dc_x\, dc_y \tag{12}$$

$$\Psi^2(z, c_z, t) = \frac{1}{\pi M_{12}}\int_{-\infty}^{+\infty}\int_{-\infty}^{+\infty} \left(\frac{c_x^2 + c_y^2}{M_{12}} - 1\right) h^2(z, \mathbf{c}, t)\, e^{-(c_x^2+c_y^2)/M_{12}}\, dc_x\, dc_y \tag{13}$$

and the macroscopic perturbed density ρ^s, velocity v_z^s and temperature τ^s as

$$\rho^1(z, t) = \frac{1}{\sqrt{\pi}}\int_{-\infty}^{+\infty} H^1\, e^{-c_z^2}\, dc_z \tag{14}$$

$$\rho^2(z, t) = \frac{1}{\sqrt{\pi M_{12}}}\int_{-\infty}^{+\infty} H^2\, e^{-c_z^2/M_{12}}\, dc_z \tag{15}$$

$$v_z^1(z, t) = \frac{1}{\sqrt{\pi}}\int_{-\infty}^{+\infty} c_z\, H^1\, e^{-c_z^2}\, dc_z \tag{16}$$

$$v_z^2(z, t) = \frac{1}{\sqrt{\pi M_{12}}}\int_{-\infty}^{+\infty} c_z\, H^2\, e^{-c_z^2/M_{12}}\, dc_z \tag{17}$$

$$\tau^1(z, t) = \frac{1}{\sqrt{\pi}}\int_{-\infty}^{+\infty} \frac{2}{3}\left[(c_z^2 - 1/2)\, H^1 + \Psi^1\right] e^{-c_z^2}\, dc_z \tag{18}$$

$$\tau^2(z,t) = \frac{1}{\sqrt{\pi M_{12}}} \int_{-\infty}^{+\infty} \frac{2}{3} \left[\left(\frac{c_z^2}{M_{12}} - \frac{1}{2} \right) H^2 + \Psi^2 \right] e^{-c_z^2/M_{12}} \, dc_z \tag{19}$$

Notice that, one can reduce to the case of a single monatomic gas (that is, the equations for the pair (H^1, Ψ^1) coincide with the ones for (H^2, Ψ^2)) if $M_{12} = 1$, $\Gamma^1 = \Gamma^2$ and $\Theta_{12} = 1$, hence only if $n_0^1 = n_0^2$ and the two gases share even the same viscosity $\eta^1 = \eta^2$.

Assuming the diffuse scattering of gaseous particles on both walls (i.e., the reemitted molecules are diffused with a Maxwellian distribution described by the wall properties), the linearized boundary conditions read as [4]

$$H^1(z = -\delta/2, c_z, t) = (\sqrt{\pi} + 2\, c_z)\, U_w$$
$$-2 \int_{\tilde{c}_z < 0} d\tilde{c}_z \, \tilde{c}_z \, e^{-\tilde{c}_z^2} \, H^1(z = -\delta/2, \tilde{c}_z, t) \quad c_z > 0 \tag{20}$$

$$H^2(z = -\delta/2, c_z, t) = \left(\sqrt{\frac{\pi}{M_{12}}} + \frac{2\, c_z}{M_{12}} \right) U_w$$
$$-\frac{2}{M_{12}} \int_{\tilde{c}_z < 0} d\tilde{c}_z \, \tilde{c}_z \, e^{-\tilde{c}_z^2/M_{12}} \, H^2(z = -\delta/2, \tilde{c}_z, t) \quad c_z > 0 \tag{21}$$

$$\Psi^1(z = -\delta/2, c_z, t) = \Psi^2(z = -\delta/2, c_z, t) = 0 \qquad c_z > 0 \tag{22}$$

$$H^1(z = \delta/2, c_z, t) = 2 \int_{\tilde{c}_z > 0} d\tilde{c}_z \, \tilde{c}_z \, e^{-\tilde{c}_z^2} \, H^1(z = \delta/2, \tilde{c}_z, t) \qquad c_z < 0 \tag{23}$$

$$H^2(z = \delta/2, c_z, t) = \frac{2}{M_{12}} \int_{\tilde{c}_z > 0} d\tilde{c}_z \, \tilde{c}_z \, e^{-\tilde{c}_z^2/M_{12}} \, H^2(z = \delta/2, \tilde{c}_z, t) \qquad c_z < 0 \tag{24}$$

$$\Psi^1(z = \delta/2, c_z, t) = \Psi^2(z = \delta/2, c_z, t) = 0 \qquad c_z < 0 \tag{25}$$

where $\delta = d/(v_0^1 \theta_1)$ is the dimensionless distance between the channel walls as well as the rarefaction parameter of the species $s = 1$, while U_w is the dimensionless wall velocity given by $U_w(t) = U_0 \, \sin(\omega\, t)$ with $U_w = U_w'/v_0^1$, $U_0 = U_0'/v_0^1$, $\omega = \theta_1\, \omega'$, $T = 2\pi/\omega = T'/\theta_1$. The time-dependent problem described by Eqs. (3)-(6), with boundary conditions given by Eqs. (20)-(25), has been numerically solved by a deterministic finite-difference method presented in detail in [4].

In order to investigate more deeply the influence of the parameters peculiar to a binary gaseous mixture, such as the molecular mass ratio, M_{12}, and the macroscopic collision frequencies ratio, Θ_{12}, on the sound wave propagation, it is convenient to derive a system of integral equations for the macroscopic fields of interest. Since the vibrations of the lower wall of the microchannel are generated by a time-harmonic forcing (of frequency ω), we introduce the following expression $U_w = U_0\, e^{i\,\omega t}$ in Eqs. (20) and (21) and then we look for solutions of Eqs. (3)-(6) under the form

$$H^s(z, c_z, t) = \mathcal{H}^s(z, c_z)\, e^{i\,\omega\, t} \qquad s = 1, 2$$

$$\Psi^s(z, c_z, t) = \Psi^s(z, c_z)\, e^{i\,\omega\, t} \qquad s = 1, 2.$$

By integrating the resulting equations along the trajectories of the molecules, we obtain an explicit expression for the distribution functions $\mathcal{H}^s$, Ψ^s, which should be inserted in the definitions (14)-(19). Thus, the integral equations for the bulk velocities of the gas components (which are the

macroscopic fields of interest in view of our subsequent considerations) read [6]:

$$
\begin{aligned}
\mathrm{v}_z^1(z) = v_z^1(z,t)e^{-i\,\omega\,t} &= \mathcal{K}_1(z,\gamma) \\
+\frac{1}{\sqrt{\pi}}\int_{-\delta/2}^{\delta/2} ds \varrho^1(s)\, sgn(z-s)\, T_0(|z-s|\,\gamma) & \\
-\frac{1}{\sqrt{\pi}}\int_{-\delta/2}^{\delta/2} ds\, \varrho^1(s)\, \mathcal{K}_2(z,s,\gamma) & \\
+\frac{2}{\sqrt{\pi}}\int_{-\delta/2}^{\delta/2} ds\, [(1-\Gamma^1)\,\mathrm{v}_z^1(s) + \Gamma^1\,\mathrm{v}_z^2(s)]\, T_1(|z-s|\,\gamma) & \\
-\frac{1}{\sqrt{\pi}}\int_{-\delta/2}^{\delta/2} ds\, [(1-\Gamma^1)\,\mathrm{v}_z^1(s) + \Gamma^1\,\mathrm{v}_z^2(s)]\, \mathcal{K}_3(z,s,\gamma) & \\
+\frac{1}{\sqrt{\pi}}\int_{-\delta/2}^{\delta/2} ds \left[\left(1-\frac{2\,\Gamma^1\,M_{12}}{(1+M_{12})}\right)\tau^1(s) + \frac{2\,\Gamma^1\,M_{12}}{(1+M_{12})}\,\tau^2(s)\right] & \\
\times sgn(z-s)\,[T_2(|z-s|\,\gamma) - \tfrac{1}{2}T_0(|z-s|\,\gamma)] & \\
-\frac{4}{\sqrt{\pi}}\int_{-\delta/2}^{\delta/2} ds \left[\left(1-\frac{2\,\Gamma^1\,M_{12}}{(1+M_{12})}\right)\tau^1(s) + \frac{2\,\Gamma^1\,M_{12}}{(1+M_{12})}\,\tau^2(s)\right] \mathcal{K}_4(z,s,\gamma) &
\end{aligned}
\tag{26}
$$

$$
\begin{aligned}
\mathrm{v}_z^2(z) = v_z^2(z,t)e^{-i\,\omega\,t} &= \mathcal{K}_1(z,\tilde{\gamma}) \\
+\frac{\Theta_{12}}{\sqrt{\pi}}\int_{-\delta/2}^{\delta/2} ds \varrho^2(s)\, sgn(z-s)\, T_0(|z-s|\,\tilde{\gamma}) & \\
-\frac{\Theta_{12}}{\sqrt{\pi}}\int_{-\delta/2}^{\delta/2} ds\, \varrho^2(s)\, \mathcal{K}_2(z,s,\tilde{\gamma}) & \\
+\frac{2\,\Theta_{12}}{\sqrt{\pi\,M_{12}}}\int_{-\delta/2}^{\delta/2} ds\, [(1-\Gamma^2)\,\mathrm{v}_z^2(s) + \Gamma^2\,\mathrm{v}_z^1(s)]\, T_1(|z-s|\,\tilde{\gamma}) & \\
-\frac{\Theta_{12}}{\sqrt{\pi\,M_{12}}}\int_{-\delta/2}^{\delta/2} ds\, [(1-\Gamma^2)\,\mathrm{v}_z^2(s) + \Gamma^2\,\mathrm{v}_z^1(s)]\, \mathcal{K}_3(z,s,\tilde{\gamma}) & \\
+\frac{\Theta_{12}}{\sqrt{\pi}}\int_{-\delta/2}^{\delta/2} ds \left[\left(1-\frac{2\,\Gamma^2}{(1+M_{12})}\right)\tau^2(s) + \frac{2\,\Gamma^2}{(1+M_{12})}\,\tau^1(s)\right] & \\
\times sgn(z-s)\,[T_2(|z-s|\,\tilde{\gamma}) - \tfrac{1}{2}T_0(|z-s|\,\tilde{\gamma})] & \\
-\frac{4\,\Theta_{12}}{\sqrt{\pi}}\int_{-\delta/2}^{\delta/2} ds \left[\left(1-\frac{2\,\Gamma^2}{(1+M_{12})}\right)\tau^2(s) + \frac{2\,\Gamma^2}{(1+M_{12})}\,\tau^1(s)\right] \mathcal{K}_4(z,s,\tilde{\gamma}) &
\end{aligned}
\tag{27}
$$

where $\gamma = (1 + i\,\omega)$, $\tilde{\gamma} = (\Theta_{12} + i\,\omega)/\sqrt{M_{12}}$, and the symbols $\mathcal{K}_i$ ($i = 1, \ldots, 4$) stand for expressions involving products of the Abramowitz functions T_n [6] defined by

$$
T_n(x) := \int_0^{+\infty} s^n\, e^{-s^2 - x/s}\, ds. \tag{28}
$$

Beyond the macroscopic fields given by Eqs. (14)-(19), a further quantity of interest in the present problem is the perturbation of the global normal stress P_{zz} (this is the quantity that is measured experimentally) evaluated at $z = -\delta/2$, since it gives the force exerted by the gaseous mixture on the moving wall of the channel. In the frame of our linearized analysis, the normal component of the stress tensor of the mixture is defined in terms of the single component parameters as $P_{zz} = P^1_{zz} + P^2_{zz}$ where

$$P^1_{zz}(z,t) = \frac{1}{\sqrt{\pi}} \int_{-\infty}^{+\infty} c_z^2 \, H^1 \, e^{-c_z^2} \, dc_z \tag{29}$$

$$P^2_{zz}(z,t) = \frac{1}{\sqrt{\pi M_{12}}} \int_{-\infty}^{+\infty} c_z^2 \, H^2 \, e^{-c_z^2/M_{12}} \, dc_z \tag{30}$$

The normal stress time-dependence is of the following known form

$$|P_{zz}| \, \sin(\omega \, t + \phi) \tag{31}$$

where $|P_{zz}|$ is the amplitude and ϕ the phase. In general, the amplitude of the time-dependent macroscopic fields is extracted from our numerical results as half the vertical distance between a maximum and the nearest minimum appearing in the temporal evolution of the macroscopic quantity.

3 RESULTS AND DISCUSSION

The results presented here refer to the noble gaseous mixtures of He-Xe (that is, helium with molecular mass $m^1 = 4.0026\, au$ and xenon with molecular mass $m^2 = 131.29\, au$) and Ne-Ar (that is, neon with molecular mass $m^1 = 20.179\, au$ and argon with molecular mass $m^2 = 39.948\, au$). For a single component gas, it has been pointed out in [7] that above a certain frequency of oscillation of the lower wall of the channel, the sound waves propagating through the gas are trapped in the gaps between the moving elements and the fixed boundaries of the microdevice. In particular, Desvillettes and Lorenzani (2012) found a scaling law (valid for all Knudsen numbers) that predicts a resonant response of the system when the dimensionless distance between the channel walls (measured in units of the oscillation period of the moving plate), $L = \frac{\delta}{T}$, takes a well-defined fixed value. In [7], the values of L corresponding to the main resonances have been analytically derived: $L_a \simeq 0.21$ (antiresonance), $L_r \simeq 0.48$ (resonance). Physically, the origin of this phenomenon can be traced back to the constructive interference (resonance) or destructive interference (antiresonance) occurring between the incident and reflected sound waves. Corresponding to a resonant response of the system, the amplitude of P_{zz} at $z = -\delta/2$ reaches its maximum value (resonance) or its minimum value (antiresonance). The occurrence of an antiresonance is particularly important since if the device is operated close to the corresponding frequency, the damping due to the gas is considerably reduced.

In figures 1-3, we report the profiles of the global normal stress amplitude at the oscillating wall, obtained by numerical integration of Eqs. (3)-(6), as a function of the period T, for three different values of the rarefaction parameter δ. We have included in these pictures the results of numerical calculations for the mixtures He-Xe and Ne-Ar with the same molar concentrations ($N_{12} = 1$), as well as those corresponding to a single component gas. Figures 1-3 reveal that, in the near-free molecular flow regime ($\delta = 0.1$) and in the transitional region ($\delta = 1$), the resonant response of the system occurs also for both gas mixtures considered (although the scaling law found for a single component gas does not hold any longer), while, in the near-continuum regime ($\delta = 10$), the propagation of sound waves in the disparate-mass He-Xe mixture does not show up any resonance.

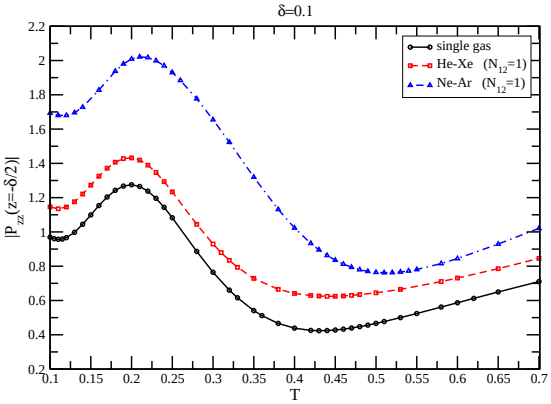

Figure 1: Amplitude of the normal stress tensor P_{zz} at the oscillating wall versus T.

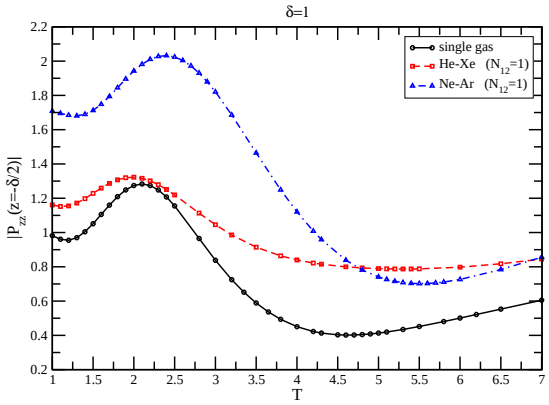

Figure 2: Amplitude of the normal stress tensor P_{zz} at the oscillating wall versus T.

In order to inspect more deeply the physical processes going on in both gas mixtures, we report in figures 4-5 the velocity profile of the mixture components as a function of the distance across the gap of the channel (at different stages during a period of oscillation). We have included in these pictures the results of numerical calculations for the mixtures He-Xe and Ne-Ar with the same molar concentrations ($N_{12} = 1$), for $\delta = 10$, when the period T matches the main resonant response of the system. In the pictures 4-5, the lightest component of each mixture has been labelled with the superscript 1, while the heaviest one with the superscript 2.

In the case of the Ne-Ar mixture, both species have the same macroscopic velocity which takes the form of a standing wave, as it happens for a single gas when a resonant response of the system occurs. On the contrary, for the He-Xe mixture, two different forced-sound modes are simultaneously present: a fast and a slow wave. The slow wave is a damped soundlike mode primarily carried by the Xe, while the fast wave should be associated to the He-component of the mixture. The fast wave in He is not analogous to a sound wave in a pure monatomic gas, since v_z^1 does not take any

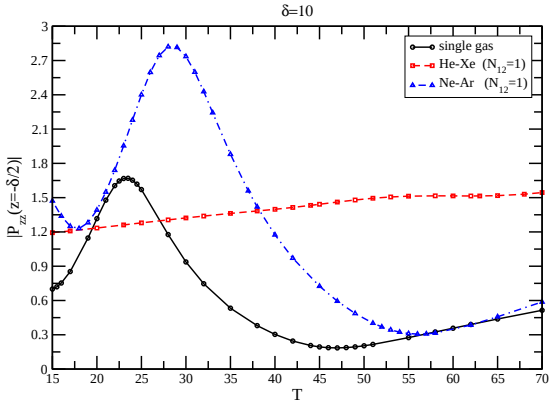

Figure 3: Amplitude of the normal stress tensor P_{zz} at the oscillating wall versus T.

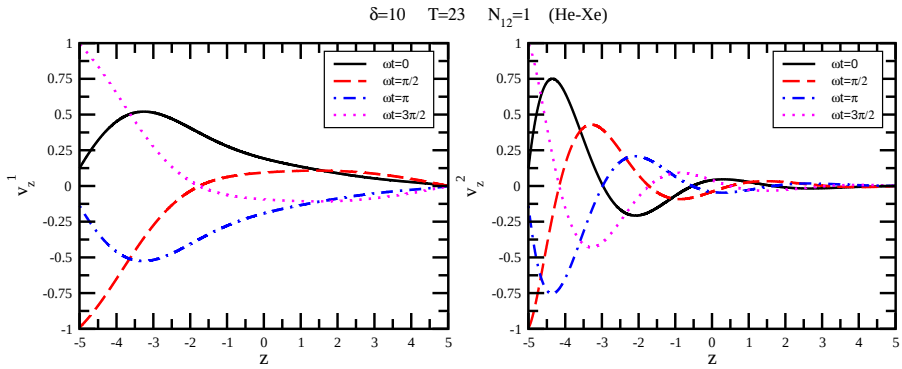

Figure 4: Variation of the macroscopic velocities of the He-Xe mixture components, in the z-direction across the gap of the channel.

longer the form of a standing wave, whatever T one chooses.

In spite of the complex form assumed by the integral equations (26)-(27), some qualitative properties on the behaviour of the two species of the mixtures can be deduced. In the near-continuum regime ($\delta \geq 10$), for mixtures like Ne-Ar, whose constituents have comparable molecular mass such that $\gamma \simeq \tilde{\gamma}$, $\Theta_{12} \simeq 1$, $M_{12} \simeq 1$, the macroscopic profiles of the two species are symmetric by interchanging the superscript 1 and 2 (as the numerical results reported in Fig. 5 show). In this case, Eq. (26) reduces to the equation for the velocity field of a single-component gas [7], since the terms $(-\Gamma^1 \, \mathrm{v}_z^1)$ and $(\Gamma^1 \, \mathrm{v}_z^2)$ cancel out as well as the terms: $-\left[\frac{2\,\Gamma^1\,M_{12}}{(1+M_{12})}\right]\tau^1$ and $\left[\frac{2\,\Gamma^1\,M_{12}}{(1+M_{12})}\right]\tau^2$. All the remarks done in [7] on the appearance of resonances/antiresonances will continue to apply, except that now, for a mixture, the phenomenon of constructive/destructive interference will involve incident and reflected waves associated to two species (since the profiles of v_z^1 and v_z^2 are symmetric). Therefore, the location of the main resonance (antiresonance) will be different from that found

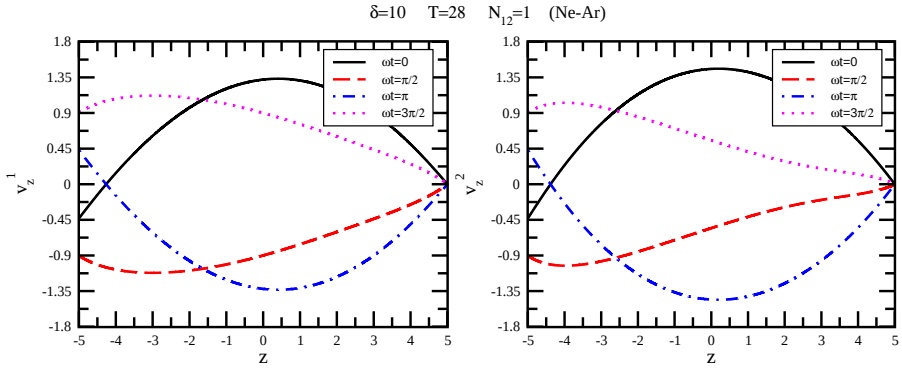

Figure 5: Variation of the macroscopic velocities of the Ne-Ar mixture components, in the z-direction across the gap of the channel.

for a single gas. On the contrary, for disparate-mass gas mixtures like He-Xe, with $\Theta_{12} << 1$, $M_{12} << 1$, $\gamma \neq \tilde{\gamma}$, the field v_z^2 approaches zero rapidly as function of z, since the Abramowitz functions involved depend only on $\tilde{\gamma}$ (whose real and imaginary parts are higher than those of γ). In this case, since v_z^2 is a rapidly damped profile, the terms $(-\Gamma^1\,\mathrm{v}_z^1)$ and $(\Gamma^1\,\mathrm{v}_z^2)$ in Eq. (26) do not cancel out and the velocity field of the lightest species v_z^1 differs in this respect from that of a single-component gas (Eq. (67) in [7]). When $\Gamma^1 \rightarrow 0$, that is for $N_{12} >> 1$, Eq. (26) reduces to the equation for the velocity field of a single-component gas and the resonant phenomenon can be observed, in the near-continuum regime, also for a disparate-mass gas mixture. This is shown in Fig. 6, where we report the profile of the global normal stress amplitude at the oscillating wall as a function of the period T, for the He-Xe mixture, when $N_{12} = 9$. The corresponding velocity profiles of the mixture components, obtained for a period T matching the main resonant response of the system, have been included in Fig. 7.

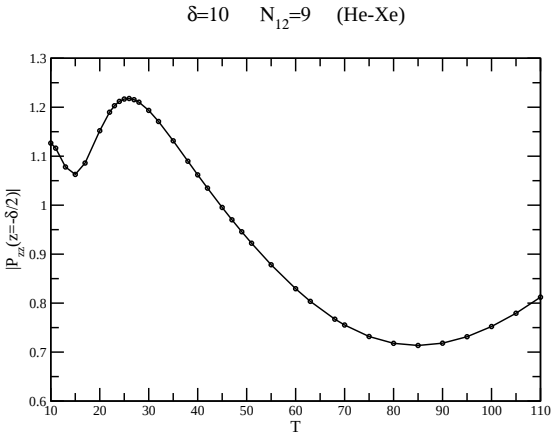

Figure 6: Amplitude of the normal stress tensor P_{zz} at the oscillating wall versus T.

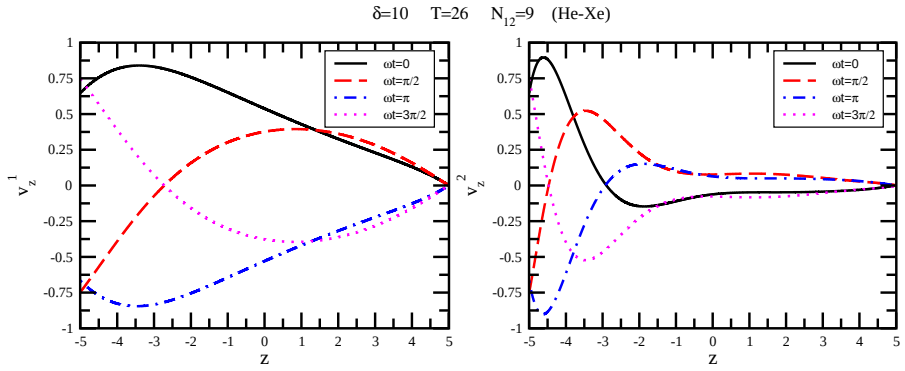

Figure 7: Variation of the macroscopic velocities of the He-Xe mixture components, in the z-direction across the gap of the channel.

References

[1] Bircumshaw, B., Liu, G., Takeuchi, H., King, T.-J., Howe, R., O'Reilly, O. and Pisano, A., "The radial bulk annular resonator: towards a $50\,\Omega$ RF MEMS filter," in *Proc. 12th International Conference on Solid State Sensors, Actuators and Microsystems* Boston, June 8-12 (2003).

[2] Pourkamali, S., Hao, Z. and Ayazi, F., "VHF Single Crystal Silicon Capacitive Elliptic Bulk-Mode Disk Resonators- Part II: Implementation and Characterization," *Journal of Microelectromechanical Systems*, **13**, 1054-1062 (2004).

[3] Clark, J. R., Hsu, W.-T., Abdelmoneum, M. A. and Nguyen, C. T.-C., "High-Q UHF Micromechanical Radial-Contour Mode Disk Resonators," *Journal of Microelectromechanical Systems*, **14**, 1298-1310 (2005).

[4] Bisi, M. and Lorenzani, S., "Damping forces exerted by rarefied gas mixtures in micro-electro-mechanical system devices vibrating at high frequencies," *Interfacial Phenomena and Heat Transfer*, **2(3)**, 253-263 (2014).

[5] Chapman, S. and Cowling, T. G., *The Mathematical Theory of Non-uniform Gases*, Cambridge University Press, Cambridge (1970).

[6] Bisi, M. and Lorenzani, S., "High-frequency sound wave propagation in binary gas mixtures flowing through microchannels," *submitted* (2015).

[7] Desvillettes, L. and Lorenzani, S., "Sound wave resonances in micro-electro-mechanical systems devices vibrating at high frequencies according to the kinetic theory of gases," *Physics of Fluids*, **24**, 092001-24 (2012).